8517-007

LOW CYCLE THERMAL FATIGUE AND FRACTURE OF REINFORCED PIPING

W.J. O'Donnell, J.M. Watson
O'Donnell & Associates, Inc.
Pittsburgh, Pennsylvania, USA

W.B. Mallin, J.R. Kenrick
Eckert, Seamans, Cherin & Mellott
Pittsburgh, Pennsylvania, USA

ABSTRACT

A large diameter steel pipe reinforced by stiffening rings with saddle supports was subjected to thermal cycling as the system was started up, operated and shut down. The pipe sustained local buckling and cracking, then fractured during the first five months' operation. Failure was due to low cycle fatigue and fast fracture caused by differential thermal expansion stresses. Thermal lag between the stiffening rings welded to the outside of the pipe and the pipe wall itself resulted in large radial and axial thermal stresses at the welds. Redundant tied down saddle supports in each segment of pipe between expansion joints restrained pipe arching due to circumferential temperature variations, producing large axial thermal bending stresses. Thermal cycling of the system initiated fatigue cracks at the stiffener rings. When the critical crack size was reached, fast fracture occurred. The system was redesigned by eliminating the redundant restraints which prevented axial bowing, and by modifying the stiffener rings to permit free radial thermal breathing of the pipe. Expert testimony was also provided in litigation resulting in a court decision requiring the designers of the original system to pay damages to the furnace owner.

THE PIPE WHICH FAILED was an exhaust duct in an emission control system at a plant in Washington state. There are a pair of submerged arc electric furnaces at the site, with parallel exhaust systems running generally east/west from the furnaces to a baghouse, as shown on Figure 1. These furnaces burn a mixture of wood chips, bituminous coal and coke. In each system, exhaust gases are drawn from the furnace up through three stacks which converge into a single duct. The gases pass through the duct to a spark box, then through loop coolers to the baghouse. There, particulate material is removed from the gas which is then vented to the atmosphere.

The north furnace is a silicon metal furnace, the south is a ferrosilicon furnace. The ferrosilicon furnace was operated at increasing power levels for almost five months; at which time large cracks occurred at many locations on the south exhaust duct, creating a safety hazard and forcing a shutdown of the furnace.

At the time of the failure of the south exhaust duct, the north duct hadn't yet been placed into service. It was necessary to determine what modifications should be made to the north duct so that it could be operated without experiencing failure similar to that of the south duct. It was also necessary to determine what repairs or modifications to the south duct would be required to put it safely back into service. A failure analysis of the south duct was performed consisting of an analytical fatigue and fracture evaluation, combined with visual and fractographic examination of the duct. The results showed that failure was caused by low cycle thermal fatigue. The thermal stresses were caused by the duct stiffening rings and redundant saddle supports which did not allow for thermal expansion of the duct. In the duct design, stiffening rings, welded to the outside of the duct, prevented free thermal expansion of the duct in the radial and axial directions. The design included saddle supports between the end supports at the expansion joints of each segment of duct. These redundant supports prevented free thermal bending of the duct.

Since high thermal stresses were caused by these improper constraints, they were removed in modifying the north duct which had not yet been put into service. The south duct had undergone very extensive low cycle thermal fatigue damage and cracking. It was therefore necessary to have it torn down and rebuilt without rings or redundant saddle supports. Both ducts have since operated eight years without any cracking

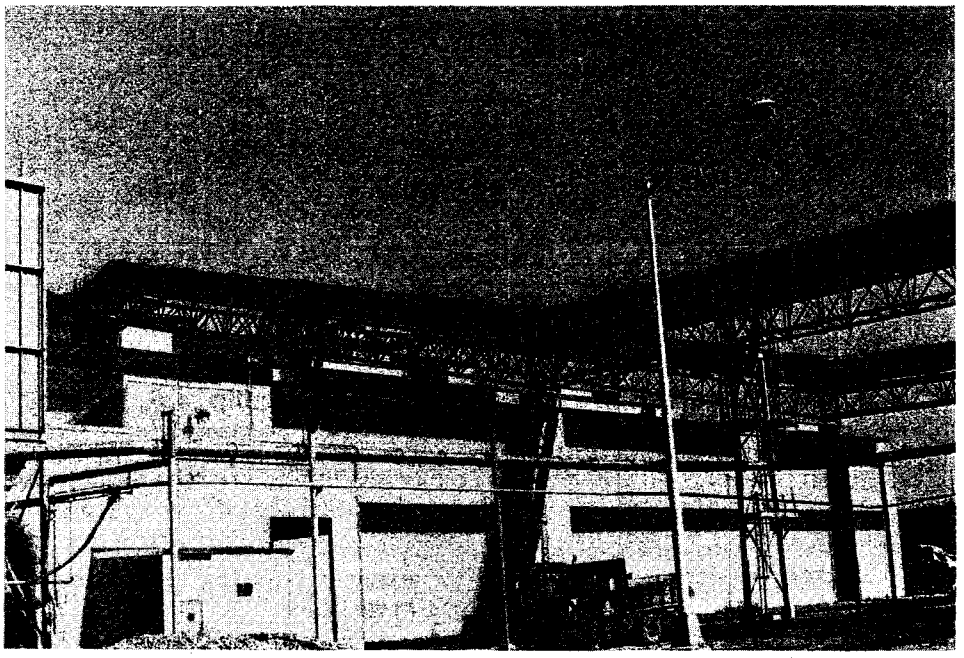

Fig. 1 - North duct viewed from just north of baghouse. Damaged south duct can be seen in background.

problems. Moreover, this operation has been above the power levels and temperatures which caused the failure in five months.

Detailed failure analyses of the south duct were performed to quantify the stress levels and failure mode evaluation. Dead weight and thermal stress analyses and low cycle fatigue analyses of the duct with its support structure were carried out. Metallurgical and fracture studies were performed to determine whether there were any material deficiencies, corrosion problems, fabrication defects or abnormal operating temperatures which may have contributed to the failures. Operating data were examined in order to determine the temperatures at which the duct had been operated. Finally, the original design calculations were reviewed to determine why the thermal stress problems were not recognized at the time of the original design.

The evaluations, examinations, and calculations which were performed are discussed in more detail in the remainder of this paper. The results showed that the duct was operated well within the anticipated temperature ranges, and that there were no fabrication defects or corrosion problems which were of significance in causing the duct failure. The failure was caused by low cycle thermal fatigue directly attributable to the use of stiffening rings welded to the duct, and to the use of intermediate redundant saddle supports in the duct segments between saddle supports at the expansion joints. When the critical crack size was reached, fast fracture occurred, ultimately producing crack lengths comparable to the duct diameter.

BACKGROUND

The emission control system for the silicon metal and ferrosilicon furnaces at the Washington state plant was designed and built over a period of about three years. The ferrosilicon south duct furnace was first operated at low power on January 10, 1976. Even at low power levels which were used in the early weeks of the system operation, the duct reportedly arched in response to circumferentially nonuniform thermal expansion. As the power increased, the temperature differences and thermal bending also increased. Because of the thermal bending, saddle support holddown bolts began breaking in February. The nonuniform temperatures were caused by several factors including flue gas impingement, weather conditions, nonuniform heat convection from the outside surface of the duct, and a build-up of insulating dust on the upper inside surface of the duct.

In early March, an insulation blanket was placed atop a portion of the duct in an attempt to raise the temperature at the top of the duct to a value comparable to that at the bottom. This reduced the arching but caused local buckling. Even with reduced arching, by early April some additional holddown bolts had failed and keepers had been bent at the duct supports. In late May, a large crack was discovered under the insulation midway between two supports at a local buckle in the duct wall. This crack was repaired by cutting out the cracked region and welding on a patch.

The system was restarted and major cracks developed in many sections of the duct: one on May 30, and several more on the morning of June 2, 1976. By June 2, cracks had propagated to

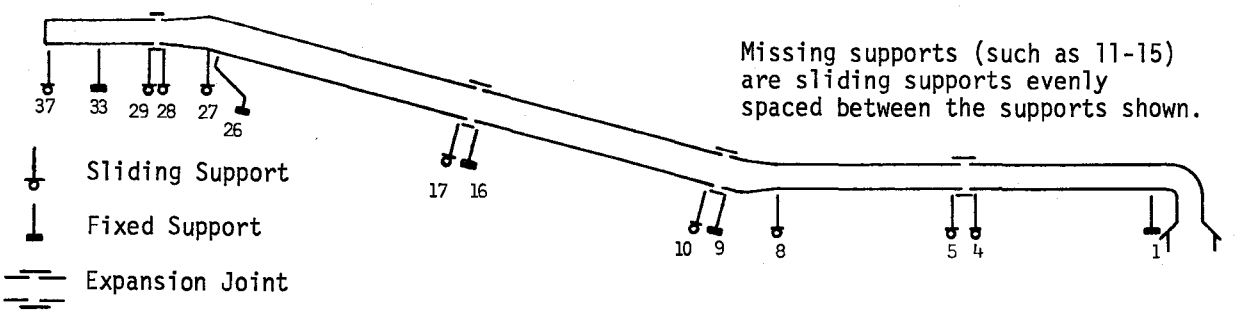

Fig. 2 - Schematic representation of the south duct showing supports and expansion joints.

the extent that the system could not safely be operated and required major repairs and modifications.

DESIGN CONDITIONS - The ductwork was designed for 100,000 hours operation (equivalent to 11.4 years continuous operation). Normal furnace operation was defined for forty-eight weeks per year as producing gas temperatures which would not exceed 704°C (1300°F) and duct wall temperatures which would not exceed 482°C (900°F) at the stack area.

An upset furnace operation was also defined for the remaining four weeks per year which would produce gas temperatures which would not exceed 934°C (1714°F) and duct wall temperatures which would not exceed 632°C (1170°F) at the stack area. This upset condition was expected to occur twice a year on the average and it was judged that the condition might persist for as long as two weeks each time.

The maximum internal vacuum was defined as 15 cm (6 in.) of water at 649°C (1200°F) and 41 cm (16 in.) of water at room temperature based on full-speed fan operation with two stacks plugged or all furnace doors closed. The duct was to be assumed to operate half full of dust and was to meet ASA standards for wind, snow, and seismic loading.

ORIGINAL DESIGN - The duct was originally designed using lengths of rolled and welded COR-TEN steel plate which were butt welded together on site. As seen on Figure 2, the duct was supported by thirty-seven saddles numbered consecutively from the baghouse (cool) end of the duct. Welded to each saddle was a stiffening ring which in turn was welded to and completely encircled the duct. The saddles were mounted on a structural steel truss.

The upper inlet (hot) portion of the duct is horizontal, with an inside diameter (ID) of 2.2 meters (7.25 feet). Each of the three furnace stacks has a refractory lined pipe with an ID of 1.8 meters (6 feet) which leads into this part of the duct. The duct has a 1.9 cm (0.75 in.) wall thickness over the first 5.2 meters (16.9 feet), a 1.3 cm (0.5 in.) wall thickness over the next 4.9 meters (16 feet) and in the first expansion joint, which is 1.3 meters (4.3 feet) long. Then there is a section 4 meters (13 feet) long with a 1.9 cm (0.75 in.) wall thickness in which the duct ID expands to 2.7 meters (9 feet).

The sloped portion of the duct coming off the roof of the furnace building has an ID of 2.7 meters (9 feet). The initial section is a bend 1.3 meters (4.4 feet) long with a 1.9 cm (0.75 in.) wall thickness which provides the transition from the upper horizontal portion of the duct to the sloped portion. The initial straight section is 23.3 meters (76.4 feet) long followed by an expansion joint 1.8 meters (6 feet) long and another section 22.5 meters (73.6 feet) long. The duct wall is 1.3 cm (0.5 in.) COR-TEN in all of these sections. Then there is an expansion joint 1.8 meters (6 feet) long followed by another bend section 4.3 meters (14 feet) long which tapers down to an ID of 2.4 meters (8 feet) and provides the transition from the sloped portion of the duct to the lower horizontal portion. Both of these sections have 1.9 cm (0.75 in.) wall thicknesses.

The lower portion of the duct is horizontal, with an ID of 2.4 meters (8 feet) and a 0.95 cm (0.375 in.) wall thickness. There is one section 16.5 meters (54 feet) long, an expansion joint 2.1 meters (7 feet) long, and another section 16.5 meters (54 feet) long.

OPERATIONAL HISTORY - Early operation of any complex system involves numerous brief shutdowns to make adjustments and correct minor problems. The furnace operating data disclose that the ferrosilicon furnace was shut down on a number of occasions for periods of time ranging from ten minutes to several hours. Twenty of these shutdowns were routine (twelve because electric power was off, seven for scheduled maintenance, and one because coke was not available), and would have occurred independent of the newness of the system

By the time that insulation was placed atop the duct in early March to try to reduce arching, the highest duct wall temperature reading obtained from the thermocouples in the upper section of the duct was 205°C (400°F). With the insulation on, the furnace had been operated at gradually increasing power levels until keeper damage and additional holddown bolt failures were noted in early April. By April 1, the recorded upper section duct wall temperature had not exceeded 300°C (570°F).

Prior to the June 2, 1976 shutdown, the normal duct wall design operating temperature

of 482°C had been recorded only three times. The design upset condition, which produces a wall temperature of 649°C had never been attained. The maximum recorded wall temperature throughout the entire operating history was 515°C (960°F).

The accuracy of the duct wall temperature thermocouple readings was confirmed by instrumented thermal tests of April 14-16, 1976. Additionally, metallurgical examinations described later in this paper, and tests on duct samples confirmed that the duct wall temperature would have been in the temperature range recorded by the thermocouples. During fabrication and construction, large paint markings had been placed upon the duct sections to aid in erection. At the time of failure, it was observed that these paint markings remained visible. It was believed that if high temperatures had been experienced by the duct wall, the paint markings would have been evaporated and no longer visible. An experiment was performed to test this belief. A paint-bearing sample was taken from the hot end of the duct (between saddles 34 and 35), upstream from the thermocouple locations. The sample was heated to the upset duct wall temperature of 1200°F to see how long the paint could withstand elevated temperatures. In less than three hours at this inside surface temperature, no trace of paint remained. The test conclusively demonstrated that the duct walls had not spent any significant time at elevated temperature because the amount of paint loss depends upon the cumulative time at that temperature.

Operating personnel were also questioned to determine whether there had been any excursions above normal operating temperatures. It was noted that in late May 1976 the duct had been operated at 22 megawatts (29,500 horsepower) for several hours with two of the three exhaust stacks plugged. An analysis of the air flow and temperature conditions with two stacks plugged was conducted and the results showed that the total gas flow from the furnace would be reduced by less than ten percent. The resulting increase in gas temperature was small. This conclusion was verified by field measurements taken the first time the stacks plugged. A pitot tube traverse taken at the horizontal port before the dropout box showed that the gas temperature was 570°C (1058°F), more than 360°C below the design upset condition. The traverse also showed that the volume flow rate through the system with two stacks plugged was 2,034 cubic meters per minute at standard temperature and pressure (71,800 SCFM). The most important effect of the plugged stacks was therefore to increase the gas velocity in the unplugged stack which would have increased the heat transfer at local gas impingement points, thereby raising the local duct wall temperatures to a value closer to the inlet gas temperature of about 590°C (1100°F). While this would have caused some local "hot spots" near the manifold at the top of the duct, there was little effect after expansion from the stack into the main duct where the velocity was reduced to normal.

The duct had also been observed glowing at night. Since the glowing region was localized, the duct would not have been much above the minimum temperature at which it can be seen to glow. Steels are known to glow at 480°C (900°F) with an intensity which depends very strongly upon how much light is present. A test was conducted on a COR-TEN A sample from the duct which showed that the apparent color also strongly depends upon the lighting conditions. The observers judged that the COR-TEN sample first began to glow somewhere between 480°C and 495°C (900°F and 925°F) in semidarkness. Color descriptions are subjective, but each observer described the color as "orange" when viewed in semidarkness. As the amount of light was slowly increased while holding the temperature constant, each observer found that the color became more "red," until eventually it appeared to have become that color altogether. In a fully lighted room, the glow became visible around 675°C (1250°F).

REDESIGN - In modifying the silicon metal furnace (north) duct, the welded stiffener rings were cut away, and the number of saddle supports reduced from thirty-seven to ten by eliminating all redundant supports between expansion joints. Each of the ten remaining saddles was modified so that, although it supported the duct, it was not welded to the duct and did not constrict its diametral thermal expansion. In this configuration, the spans between supports were fixed by the locations of the existing expansion joints. These long spans introduced a potential problem with material creep during high temperature operation. Dead weight stresses increase with the square of the span length, and removing the redundant supports greatly increased the span length. The resulting stresses would have exceeded the elevated temperature allowable stress values, which are limited by creep effects. Therefore, a refractory lining insulation was added to keep the material at a temperature below the creep regime.

It would also have been possible to use more expansion joints in order to reduce the spans so that the dead weight stresses remained below the elevated temperature allowable stresses without using refractory lining. However, it was concluded that this option would not be as cost effective in view of the already existing hardware.

High prior fatigue damage required that the existing COR-TEN in the ferrosilicon furnace (south) duct be scrapped. The redesign required either more expansion joints or refractory lining. Cost benefit analyses were carried out, taking into account safety, reliability and maintenance factors as well as differences in fabrication costs. Such factors as outside duct temperature, duct movement, the combined effects of the small amounts of air leakage at each expansion joint, and the details of the support

structure design in the sloped region were considered. Moreover, there were distinct advantages to having identical maintenance procedures for both ducts, and benefiting from lessons learned from operating experience. Hence, it was concluded that twin duct systems would be the better design.

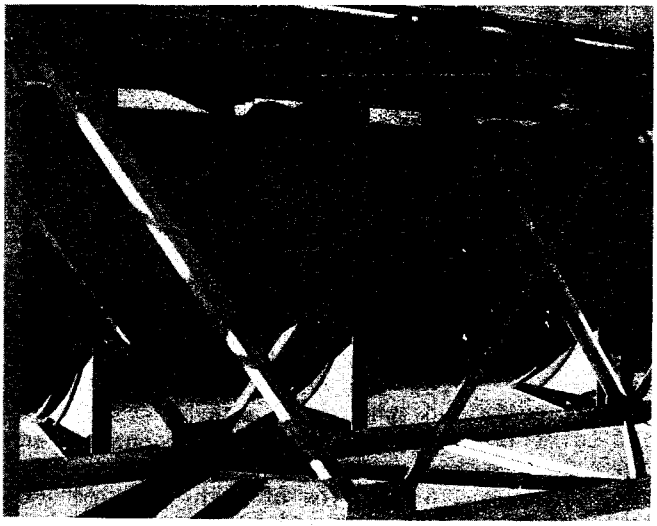

Fig. 3 - Bottom view of typical shell crack at stiffener ring

EXAMINATION OF FAILED DUCT

Although thermal stresses could not be measured during furnace operation because the system could not safely be operated in the severely cracked condition, the consequences of thermal expansion were quite evident, as can be seen on Figures 3-8. Holddown bolts attaching the fixed saddles to the support truss had failed because thermal bending of the duct was restricted by redundant restraints. Keepers which hold the sliding saddles down had also failed because of the thermal bending of the duct. The many cracks and buckles in the duct itself also attested to the presence of high thermal stresses.

The source of the high thermal stresses was readily determined by examination of the failures and the geometry of the structure. Support rings on the outside of the duct were welded to the duct preventing free diametral thermal breathing of the duct. Large temperature differences between the rings and the duct produced large differential thermal expansions between the ring and the duct in both the radial and axial directions, resulting in large thermal stresses in the duct at the welds. Weather conditions (wind, rain, snow, darkness) caused changes in heat transfer from the outside surface of the duct, resulting in cyclic thermal stresses. Predictable variations in the gas temperature due to startup, normal operation, and shutdown of the furnace also caused cyclic thermal stresses. These cyclic stress conditions produced fatigue cracks in the duct. The fatigue cracks initiated near the stiffener rings, and propagated through the duct under the influence of the thermal stresses caused by the rings and the thermal bending stresses in the duct caused by the redundant supports.

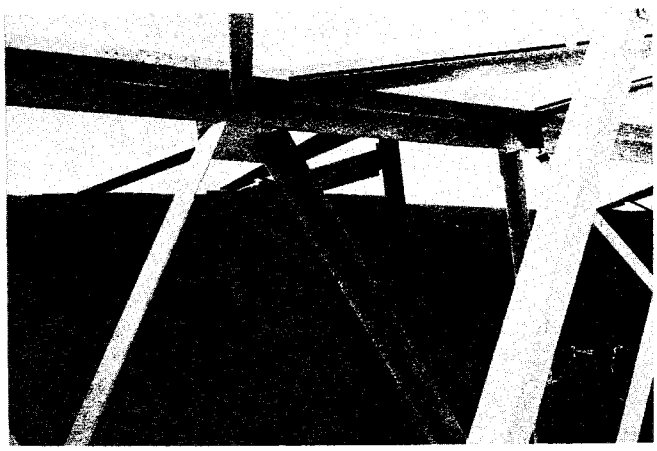

Fig. 4 - Bottom view of shell crack at stiffener ring which has propagated away from the ring

Fig. 5 - Crack propagated through the duct wall

The crack propagation was aggravated by the use of redundant supports in each segment of duct between expansion joints. Basic design to accommodate thermal expansion consists of supporting each segment of the duct system only at the end expansion joints. This allows the duct to flex without introducing large axial bending moments when the temperature distribution is nonuniform around the circumference of the duct. There are many causes of such nonuniformities including impinging gas at duct intersections or bends, weather conditions (the duct is exposed to the weather), and nonuniform dust buildup inside the duct. In the original design, several intermediate redundant supports were used in each segment of the duct. These additional

redundant supports introduced significant thermal bending loads in the duct. These loads were evident from the arching of the duct. Not only did they break holddown bolts and keepers, they also tended to open up the fatigue cracks which had been initiated at the support rings, causing them to propagate to dangerous lengths.

The midspan buckle which occurred near the circumferential butt weld midway between saddles 7 and 8 was due to locally higher temperatures which produced axial compression in the duct wall where insulation was placed on the top of the duct. Eventually, buckling produced cracking in that region.

Fig. 6 - Open Crack at stiffener ring

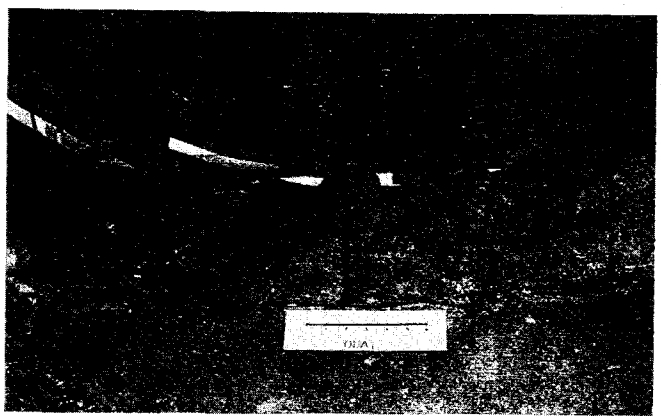

Fig. 7 - Fast fracture at stiffener ring

Fig. 8 - Midspan buckle

MATERIAL EVALUATION

Tests of the duct material were conducted, including various mechanical tests, metallurgical assessments, and chemical analyses. Metallurgical, scanning electron microscopy and electron-excited, energy-dispersive x-ray analysis examination of fracture surfaces and cross section samples were made. Such analyses were made on pieces of COR-TEN removed from the duct and also on virgin samples. Macroscopic examinations of material from the failed duct showed numerous cracks in close proximity to the intermittent welds and arc strikes. Photomicrographs indicated that most of the areas of the fracture surfaces examined were mixed mode, i.e., ductile and brittle fractures. Low cycle fatigue cracks initiated at locally high strain points and subsequently propagated as fast fractures once they had reached a critical size.

The microstructure at the hot end of the duct differed from that in unused material in that it contained spheroidized carbides. This indicates that the duct became hot enough to cause this microstructural change. Such changes are, of course, a function of both the time and temperature of exposure. The temperature had to exceed 445°C (833°F) for some period of time to cause this particular microstructural change in COR-TEN steel. The spheroidized carbides could have resulted from a long time exposure at 454°C (850°F), or from a very brief exposure at 689°C (1200°F), or from an intermediate time at a temperature between 454°C and 689°C .

According to the operating data for the main 2.7 meter diameter duct, the duct skin temperature exceeded 445°C for varying lengths of time during a two week period. The observed microstructure for a sample taken from the sloped region of the duct is consistent with the cumulative effect anticipated for these time-temperature conditions. Hotter temperatures would have been experienced in the 2.2 meters diameter duct where stack gases impinge directly against the wall. This region was observed glowing at night on several occasions. The microstructure of the sample taken from this region contains more spheroidized carbides than the other sample, consistent with the greater cumulative exposure to temperatures above 445°C in the manifold.

The fatigue properties of COR-TEN steel used in the failure analysis were verified by tests. Material which had originally been purchased for use in the duct but which was never used was soaked for 100 hours at 540°C (1000°F). This material had seen no prior strain damage. Low cycle fatigue tests were performed on this material in air at 1000°F using hourglass-shaped specimens. The axial strain was controlled in the tests to give strain ranges of 1.5%, 2.0%, 4.0% and 5.0%, respectively, based on diametral strain measurements. In addition, six hold-period tests were performed with hold periods of three

or fifteen minutes. Hold periods in tension only were employed in five of these tests while one was performed using a hold period in compression only. The fatigue tests included only very short hold times compared to the service conditions. It was not practical to run laboratory fatigue tests with hold times comparable to service conditions because it takes too long to generate the data. During hold times at elevated temperature, elastic strains are converted into creep strains, which produce much more fatigue damage in materials such as COR-TEN. Thus, for a fixed total strain range such as used in these tests, the fatigue life would be expected to be reduced with increasing hold times. The data showed this to be the case. A three minute hold time reduced the fatigue life by about a factor of two. Extrapolations to the service condition hold times on the order of days indicate quite good agreement with the theoretical failure curve at 1000°F.

The resulting low cycle fatigue test data is plotted on Figure 9, along with the theoretical mean failure curves which had previously been derived using tensile test data reported by U. S. Steel. The theoretical failure curves were based on the Langer-Coffin equation which does not include consideration of creep effects. However, the use of a relatively low reduction in area value of 34 percent was believed to account for the reduced ductility due to thermal aging and creep effects at 1000°F. Note that all of the fatigue test data falls between the theoretical failure curves for 370°C and 540°C (700°F and 1000°F),

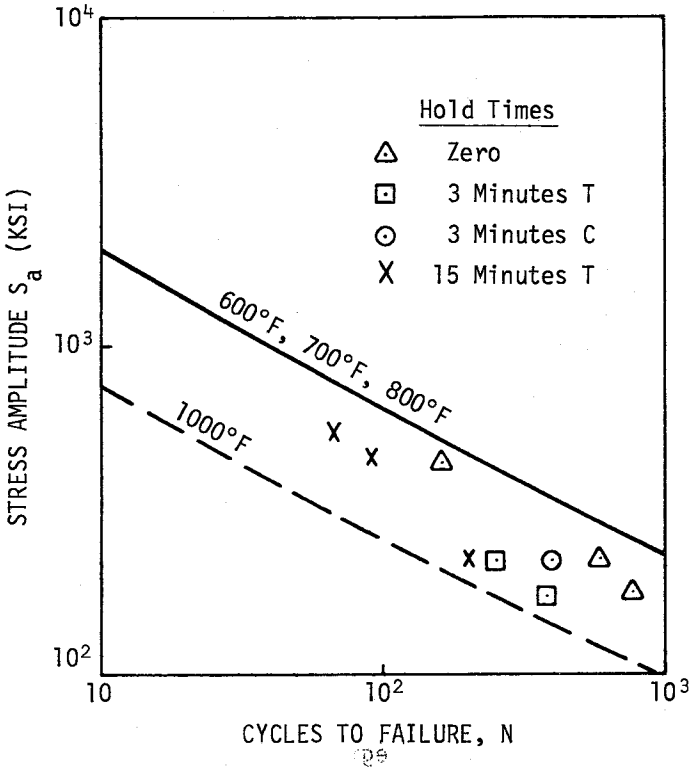

Fig. 9 - Low cycle fatigue test data

respectively. Thus, the fatigue test results indicate that the fatigue properties of COR-TEN steel are much lower at 1000°F than at 600, 700 or 800°F. Moreover, the data substantiates the validity of the fatigue properties used.

FAILURE AND REDESIGN ANALYSES

Failure analyses and redesign analyses were performed to evaluate the failure of the south duct and to assure the structural integrity and reliability of the redesigned ducts. This section summarizes those analyses.

FINITE ELEMENT ANALYSES - Temperature distributions in the duct stiffener ring were calculated based on a reference 538°C (1000°F) inlet gas temperature and corrected for other operating inlet gas temperatures. Gas temperature measurements taken at various times during furnace operation indicate that the actual gas inlet temperature at the hot end of the duct was in the range from 540°C TO 595°C (1000°F to 1100°F) during the period of south duct operation at 22 megawatts.

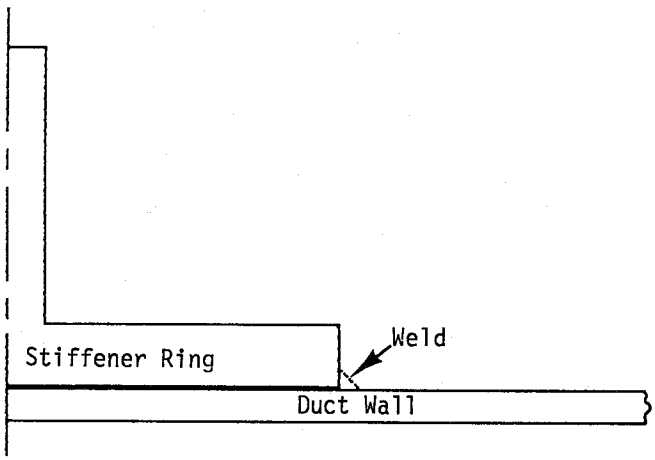

Fig. 10 - Stiffener ring welded to duct

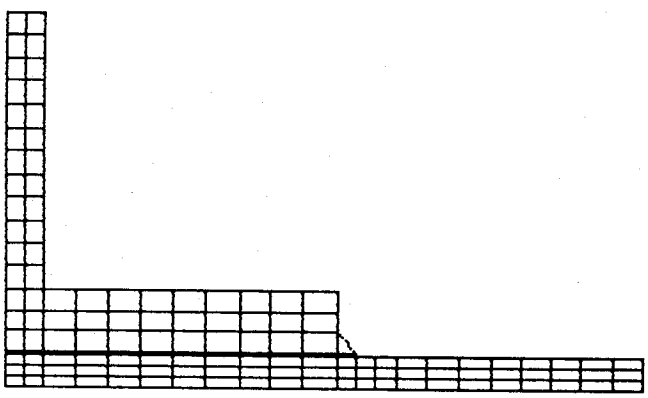

Fig. 11 - Finite element model of ring/duct interface

The computer model illustrated on Figures 10 and 11 shows a gap between the duct and the stiffener ring. Field measurements show that

this gap, which resulted from the fabrication process, varied from a minimum (usually direct contact) near the bottom of the duct to a maximum near the top of the duct. The gap is also larger at the welded edges of the ring than at the center of the ring due to the permanent anticlastic curvature introduced when the rings were fabricated. The maximum gap varied from ring to ring. A series of thermal problems were run with the gap thickness varied from zero to 2.54 cm (1 in.). The reference problem has a 0.119 cm (0.0469 in.) gap considered representative of the "typical" gap thickness around the circumference.

Thermal stresses in the duct due to the differential thermal expansion between the duct and the stiffener ring were also evaluated. Here, as in the thermal analysis, a series of problems were run with various gap thicknesses. The reference detailed analysis corresponded to the reference thermal problem. Elastically calculated stresses were far above yield, demonstrating the detrimental effect of using stiffener rings welded to the duct.

STRUCTURAL ANALYSES USING BEAM ELEMENTS - Structural analyses were performed using beam elements, employing both hand and computer calculations. The computer program employed uses linear temperature variations across a beam cross-section from top to bottom and/or from side to side. Hence, initial calculations were performed to determine an equivalent linear temperature distribution for the actual nonlinear temperature variation. The computer analyses provided the thermal bending stresses in the complex duct and support system resulting from these equivalent linear temperature variations. Again, the elastically calculated stresses were far above yield, demonstrating the detrimental effect of having redundant supports preventing thermal bending of the duct.

Thus, the computer structural model provided support reactions and thermal stresses in the duct due to the basic geometry of the duct and its support locations. Detailed local finite element stress analysis accounted for the effect of putting stiffening rings around the duct and welding them to the duct. The effects of the saddle support reactions on the duct shell were included using stress solutions available in the literature.

The results of the structural analyses of the original design showed that the flexibility of the truss increased dead weight stresses and reduced thermal bending stresses in the duct. This result was due to the improper design of the duct which incorporated redundant supports between the expansion joints. Hence, thermal bending of the duct imposed high cyclic loads and stresses on the support truss, buckling several truss members. With properly designed duct supports, thermal bending of the duct does not bend the supporting truss. Moreover, the flexibility of the truss would have no effect on either the thermal or dead weight stresses in the duct. This is important since the typical design sequence involves first designing the duct, and then using the resulting weight to design the truss.

FATIGUE ANALYSES - The calculated loads and stresses were used to perform a low cycle fatigue evaluation using the actual operating data. The operating temperatures were lower than the temperatures anticipated in the design specifications. There were no known cycles corresponding to the anticipated 934°C gas inlet temperature upset condition, and only three cycles to the normal operating temperature. Hence, the actual operating cycles were used to evaluate the fatigue damage.

Since local stresses were far in excess of the yield strength of the materials at the ring to duct stitch welds, elastic-plastic analyses were used to obtain the strain ranges needed to perform a low cycle fatigue evaluation. The evaluation was made using fatigue design curves obtained by applying a factor of twenty on cycles to the theoretical failure curves shown on Figure 9. Based on the design curves, a cumulative fatigue usage of 13 had been reached when failure occurred. This is consistent with the knowledge that cracks had initiated and grown to a critical size and propagated as fast fractures at this usage. Actual failure occurred between the design fatigue curve and the theoretical mean failure data for small polished laboratory test specimens. Failure below the mean laboratory failure curve is expected due to size effects, surface finish effects, environmental effects and scatter in the data.

FRACTURE MECHANICS ANALYSES - Exhaust gases and dust were blowing through cracks up to three meters long by the time the ferrosilicon furnace was shut down in June 1976. In order to understand why the cracks had propagated so far, fracture mechanics analyses were employed to assess crack propagation into regions well away from the stiffener rings. This behavior is a function of the stress field and the fracture toughness of the material. The elastically calculated stresses varied from far above yield at and near the stiffener rings to well below yield at midspan. Temper embrittlement associated with elevated temperature operation caused the fracture toughness K_{Ic} to vary from a minimum of 27.5 MPa$\sqrt{m}$ (25 ksi $\sqrt{in.}$) at ambient temperatures near the furnace up to five times that value for uneffected material near the duct outlet where it was not exposed to elevated temperatures. These values were obtained by applying standard correlations to Charpy V-notch test data obtained on the duct material. The cracks ran during the shutdown transient when the duct wall temperature dropped, reducing the toughness below the critical value for the existing fatigue cracks. Fast fractures moving at the speed of sound in the material were heard by the system operators.

Linear fracture mechanics is applicable to the elastic stress regions away from the stiffener rings, but not to the plastic stress

regions near the rings. Initiation of fatigue cracks occurred at the 7.6 cm (3 in.) long stitch welds attaching the stiffener rings to the duct wall. Critical crack sizes for various observed crack configurations were evaluated over the K_{IC} range for stress intensities up to yield. These evaluations showed that cracks propagating from the stiffener welds into regions at these lower stresses would have grown to critical sizes even for the unembrittled material. The critical crack sizes at yield were such that even a shallow crack the length of the stitch weld would exceed the critical size and propagate through the duct.

REVIEW OF ORIGINAL DESIGN CALCULATIONS

When the crossover duct failure became the subject of litigation, the original design calculations were reviewed to determine why the stiffening rings had been welded to the saddles and duct and why redundant supports had been used between the expansion joints. The original design was for an operating condition with a continuous gas inlet temperature of 934°C (1714°F) and a duct wall temperature of 649°C (1200°F). This wall temperature comes from the upset condition with a 17°C (30°F) margin. Axial temperature profiles for both the gas and duct wall corresponding to this operating condition were determined.

It is fundamental in designing ducts or large diameter thin-walled pipes for elevated temperature service to allow for thermal expansion. In this ductwork, expansion joints were provided to accommodate the axial thermal expansion of the duct. However, the radial thermal expansion of the duct was improperly restrained by welding stiff reinforcing rings on the outside of the duct as shown on Figure 10. Moreover, the rings were 0.26 meter (10.275 in.) wide and welded on both sides so that the thermal axial expansion under the rings also introduced large stresses at the welds. The rings were intended to keep the duct from creeping out of round due to the small vacuum pulled by the exhaust fan. However, they could have served this function as well had a small radial clearance for thermal expansion been provided between the duct and had the rings not been welded to the duct. As designed, the welded rings restrained the thermal expansion of the duct since the duct wall operates at a much higher temperature than the rings. The rings were not insulated and were exposed to atmospheric cooling. Very high thermal discontinuity stresses were therefore created in the duct material at the reinforcing rings. The thermal structural interaction between the duct and the stiffening ring and the resulting fatigue were not considered in the original design calculations.

When the stiffener rings were welded to their saddle supports to keep the duct from sliding down the slope, the problems created by the rings were amplified. Over the arc subtended by the saddle, the stiffness of the ring was increased while the effective temperature was decreased. This accentuated the radial constraint on the duct and increased the thermal stresses in the duct at the reinforcing rings. The original design calculations did not consider the effect of the saddles on the temperature distribution or on the thermal stresses in the duct, stiffening rings or saddles.

Each segment of ductwork between expansion joints should have been supported only at its ends so that the duct would have been free to bend thermally. This is a basic design consideration for such ductwork. Thermal bending is caused by impinging gases, dust build-up and nonuniform cooling on the outside wall of the duct which is exposed to the atmosphere. None of these factors were considered in the original design. When the duct is tied down between expansion joints, it is not free to arch when the top and bottom of the duct are at different temperatures. Moreover, the additional improper redundant supports impose loads on the duct by restraining the free thermal bending. The resulting loads can be many times higher than the dead weight loads. These loads tended to propagate the low

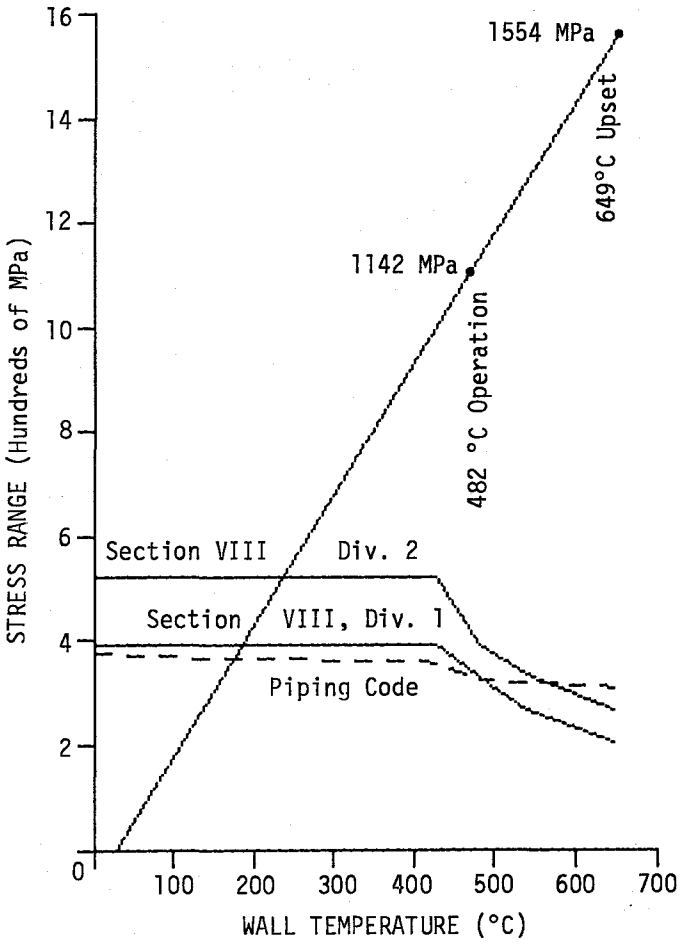

Fig. 12 - Comparison of elastically calculated stress range to limits imposed by Codes

cycle fatigue cracks which had been initiated by the welded reinforcing rings, yet had never been considered in the design calculations.

COR-TEN steel is not an ASME Boiler and Pressure Vessel Code material. However, the basis for establishing Sm described in Section VIII, Division 1 and that described in Section VIII, Division 2 of the Code were used to determine stress range limits for thermal stresses in this application. The allowable stress range formula for expansion stresses given in paragraph 102.3.2C of the ANSI B31.1 Piping Code was also considered. As can be seen on Figure 12, by the time the duct wall temperature goes above 233°C (452°F), the allowable stress range has been exceeded for all three of these approaches. Normal anticipated operation and the occasional upset condition produced elastically calculated stresses far above these limits.

Unrealistic simplifying assumptions were made in performing the original design calculations. For example, it was assumed that there would be no circumferential temperature variations around the duct even though a specified design condition included having the duct half filled with dust. Dust acts as an insulator, thereby creating temperature differences between the top and bottom of the duct. Note that there are also significant temperature differences across the duct at the bends due to gas impingement and from top to bottom due to weather conditions even if there were no dust buildup.

Commencing shortly after system shutdown, the engineers performing the failure analysis, the redesign analysis, and the material evaluation worked closely with the attorneys prosecuting the claim on behalf of the plant owner against the system designer. This team approach greatly facilitated the ultimate utilization of the analyses and material evaluation at the trial. It also assured that an appropriate and judicially admissible record supporting the engineering decisions which were made was maintained as work progressed. This minimized the potential for "second guessing" by persons in an adversary position who were challenging the failure and redesign analyses and the cost of the redesign work. The attorneys (three of whom have engineering degrees) benefited from this team approach by acquiring a better understanding of the complex engineering issues involved in the failure analysis and redesign effort. This better understanding in turn enhanced the attorneys' ability to present the expert testimony at the trial in a readily comprehensible manner.

The outcome of the lawsuit was a court determination that the duct failure was caused by defective design and multimillion dollar compensation was awarded to the plant owner.